Journal of Applied Fluid Mechanics, Vol. 17, No. 8, pp. 1705-1716, 2024.
Available online at www.jafmonline.net, ISSN 1735-3572, EISSN 1735-3645.
https://doi.org/10.47176/jafm.17.8.2512

Influence of Plasma on the Supersonic Air-intake Buzz

P. Kumar and S. Das†

Department of Space Engineering and Rocketry, Birla Institute of Technology, Mesra, Ranchi-835215, India

†*Corresponding Author Email: sudipdas@bitmesra.ac.in*

ABSTRACT

Buzz is an unwanted and inevitable phenomenon occurring due to the subcritical operation of intake which needs a comprehensive understanding. The buzz pattern in axisymmetric intakes differs from 2D counterpart and requires further investigation. The current study emphasizes the ways of buzz formation and its sustenance at supersonic speeds. In the present study URANS simulations have been done for various throttling ratios to simulate the engine demand conditions. It has been found that the onset of intake buzz happens for anything above the throttling ratio of 0.54. An active flow control technique using plasma actuator was used here to mitigate the influence of buzz. The study also emphases on the impact of plasma power densities on the intake performance.

Article History

Received December 18, 2023
Revised February 24, 2024
Accepted March 4, 2024
Available online May 29, 2024

Keywords:

Buzz
Throttling
Plasma actuator
Flow control
Supersonic intake
Axisymmetric

1. INTRODUCTION

Air intakes are an essential part which plays a crucial role in assuring the performance, stability, and overall operational success of any air breathing engine. Providing a constant, high-quality airflow with little pressure loss and distortion during a variety of flight situations, from stationary operation to supersonic speeds, presents a special set of challenges for supersonic air inlets (Mattingly & Von Ohain, 2006). Most supersonic intakes are either axisymmetric or two-dimensional.

Abedi et al. (2020) have done the simulations for the axisymmetric and three dimensional (3-D) numerical analysis for air intake at M=2, using steady state RANS equations and k-ω model. It has been found that for all operational circumstances, 3-D effects are not powerful enough to significantly affect the intake performance.

Operating conditions of supersonic intakes decides the complex flow behaviour to be existing around the air intake. Ideally supersonic intakes give maximum efficiency at critical condition where usually the normal shock is placed at the vicinity of cowl lip and the stagnation pressure loss is minimum. If the normal shock moves downstream of the intake duct it is said to be at supercritical operating condition. If the normal shock moves upstream, then the intake is said to be operating at subcritical condition (Seddon & Goldsmith, 1985).

Due to the complex flow features at supersonic flight, such as the existence of multiple shock and expansion waves, shock-boundary layer interactions (SBLI), airflow separation, and buzz instability, it becomes more challenging for an air intake to perform efficiently (Seddon & Goldsmith, 1985).

According to Ferri and Nucci (1951), buzzing starts when normal shock and oblique shock interacts with the shear layer formation from cowl that flows inside of intake at subcritical conditions. In a subsequent experiment, Dailey (1954) discovered that buzzing begins with the inception of flow separation over the spike or ramp side of the supersonic-air intake. Boundary layer bleed was introduced (Vivek & Mittal, 2009), which can be utilised to manage intake buzz. Relatively lower bleeding causes little buzz to be seen. A big buzz is seen at higher bleed. When high bleed is used, both upstream and downstream of the throat, buzz is totally removed. Lee et al. (2011) carried out experimental and computational study over rectangular and axisymmetric intakes of tiny-size. Their findings show that the buzz conditions for tiny-sized intake is alike to that of a large intake, but a separation bubble from the ramp side can readily affect a small intake.

Kwak and Lee (2013) numerically obtained buzz phenomenon over an intake experimentally tested by Nagashima et al. (1972). Variation of exit area of the intake, amounted to changes in the buzz phenomena which was also ensured through two-dimensional (2-D) as well as 3-D simulations. For a rectangular supersonic intake, Trapier et al. (2006) observed that a little buzz occurs at

NOMENCLATURE

TR	Throttling Ratio	PPD	Plasma Power Density
A_e	exit area of Intake	A_c	Capture area of intake
P_s	static pressure	$P_{0,\infty}$	Freestream total pressure
TPR	Total Pressure Ratio	FD	Flow Distortion

120 Hz and a large buzz occurs at 18 Hz. DDES simulation was carried out by Trapier et al. (2008) at M=1.8. Their findings closely resembled those of the experiment. Chen et al. (2017) stated that for design condition the two buzz phases (little and big buzz) may occur at same origin i.e. from the Ferri criterion. Further investigation of Chen et al. (2018) at over speeding mode at M=2.5, they found the medium buzz which is caused due to the bow shock which comes inside the cowl and is completely independent of little & big buzz. Chen and Tan (2019) found that medium buzz does not stays long & fades away at design Mach number (M=2). They also suggested that with the inclusion of the bleed, strong flow instability is completely eliminated. It is noticed that buzz onset are not always caused by over speeding mode.

Soltani and Sepahi-Younsi (2015) have done experiments on buzz studies in an axisymmetric intake at various Mach numbers. Their findings show that the intake duct's acoustic properties significantly influence the buzz onset. They also found that the large boundary layer separation has both little and big buzz type of instabilities. Additionally with the increment in flow Mach number buzz frequency and amplitude were decreased. Soltani et al (2016) have done experiments on bleed position in the axisymmetric air intake at various Mach number. Their finding reveals that position of the slot bleed location nearer to the normal shock has a positive effects on intake stability in the subcritical condition. Maadi and Sepahi-Younsi (2021) have done experiments on porous and slot bleed in the supersonic air intake at various Mach numbers. Their finding showed that porous bleed has upper hand comes to the TPR point of view in the supercritical condition and also flow distortion is minimum. When it comes to slot bleed it has positive effect in delaying the onset of buzz and also reducing the intensity of the buzz oscillations.

Ganiev et al. (2000) conducted the experiments and numerical studies at various Mach numbers to reduce the drag. With the introduction of hot gas & plasma injection, the drag was reduced by more than 50%.

To study the fluid movement and transfer of heat caused by glow discharges, a computational structure based on an intuitive electromagnetic model in combination with the Navier-Stokes equation is created. Simulations were run to examine the impact of the plasma's generated heat transfer. Shyy et al. (2002) have discovered that a plasma-induced jet can alter the flow pattern around it and accelerate heat transfer from the surface.

A pulsed laser beam is focused into a small focal volume to deposit laser energy into a gas performed numerically by Kandala and Candler (2004). They found that for a supersonic flow, the ideal place for energy deposition, where the pressure is decreased to its greatest extent.

Macheret et al. (2004) studied the effect of heat source which were inducted at hypersonic speed, for off design conditions. The main goal of this technique is to produce a heating zone that is upstream of and slightly below the cowl lip. The zone of elevated temperature and/or pressure would divert the incoming flow, increasing the mass flow into the intake. They found the location for the energy deposition where there was reduction in spilled air flow. Similarly the heating source and its area was also studied by Sepahi-Younsi and Esmaeili (2020). The numerical analyses were done for mixed compression air intake at design and off design conditions. By the application of heating area, they discovered that bow shock forms across the air intake and has a favourable impact on the majority of the performance measures. Patel et al. (2012) investigated the use of DBD plasma actuators to prevent flow separation induced by shocks in turbulent boundary layers. Numerical and experimental tests were conducted on a 12° wedge flow, an impinging shock using an airfoil, and a Mach 2.0 nozzle flow. The study found that while a minimum of 75 kV was needed to suppress separation bubbles, arcing issues limited the experimental results, preventing voltages from exceeding 60 kV.

Plasma actuators in the supersonic intake have been explored experimentally and computationally by Falempin et al. (2015). They found that, the production of weakly ionised plasma can regulate the primary oblique shock to sit exactly on the intake's cowl lip i.e shock on lip condition can be achieved. Numerical simulations were run in a two-dimensional rectangular intake by Ferrero (2020) with plasma actuators and bleed under off-design conditions. The outcomes demonstrated that boundary layer separation can be lowered at various plasma actuator sites and also with the combined effect of bleed and plasma, there were positive effects on performance. Numerical simulations were carried out by Kumar and Das (2023), for supersonic mixed compression axisymmetric intake at M=2. Their finding reveals the optimum location for the actuation of the plasma for buzz phenomena that can be alleviated.

It has been observed that very few studies have been performed using plasma actuators on the supersonic intake flow field. The area of intake buzz and its mitigation using plasma as a tool is quite an untouched area. However, the available studies indicate the use of plasma to counter the adverse effects of shock boundary layer interactions. The present investigation focuses on using the plasma actuators to mitigate buzz phenomena and obtain the performance benefits at subcritical operation of axisymmetric intake designed for Mach 2.

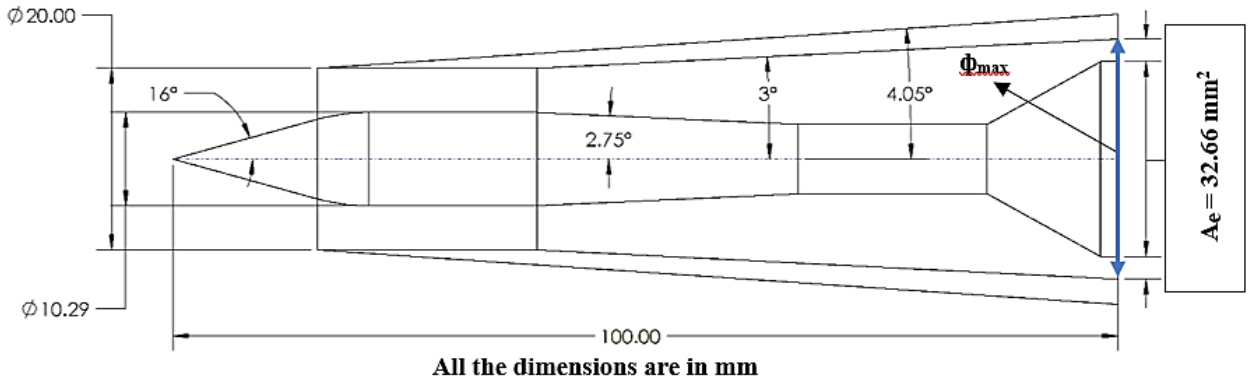

Fig. 1 Dimensional details of axisymmetric intake

2. INTAKE DESIGN

The current axisymmetric intake has been adopted from Maadi and Sepahi-Younsi (2021). The final adopted intake has been reappropriated for future experimental studies suiting the wind tunnel requirements. The design Mach number of the intake is 2, and the reappropriated dimensions has intake capture diameter of 20 mm and length of 100 mm. The spike's semi-conic angle is 16° with a maximum spike diameter of 10.29 mm and maximum diameter (ϕ_{max}) at exit as 26.44 mm, and further details is shown in Fig. 1. The total pressure and temperature is maintained at 30 Psig and 300 K, respectively. The subcritical condition is achieved by using a conical plug to change the exit area of the intake. The throttling parameter is introduced as throttling ratio (TR), which ensures the scaled area variation at the intake exit.

$$TR = 1 - \frac{A_e}{A_c} \quad (1)$$

Here, TR of 1 represents that the throttling plug entirely blocks the exit area, whereas TR of 0 represents that the plug is fully open and corresponds to an area nearing to the capture area of intake.

2.1 Numerical Methods

For axisymmetric numerical simulations to represent the general flow features of air intake, Ansys Fluent® commercial software has been used. Unsteady, Reynolds Averaged Navier Stokes (URANS) equations have been solved with k-ω SST turbulence closure model. The internal duct and the region surrounding the cowl lip have been included in the solution domain with the proper boundary conditions in order to shorten the calculation time. A standard grid distribution has been selected using uniformly distributed quadrilateral cells as shown in Fig. 2. By keeping a minimum spacing of 0.01 in the y direction close to the wall, it was possible to attain the y^+ value of less than 5. A density-based solver with second order implicit scheme is adopted. The Flux splitting method used is AUSM (Advection Upstream Splitting Method). Courant number is set to 0.8. Figure 2 also indicates the different boundary conditions and the overall domain used in the present study. Points P1 and P2 are the

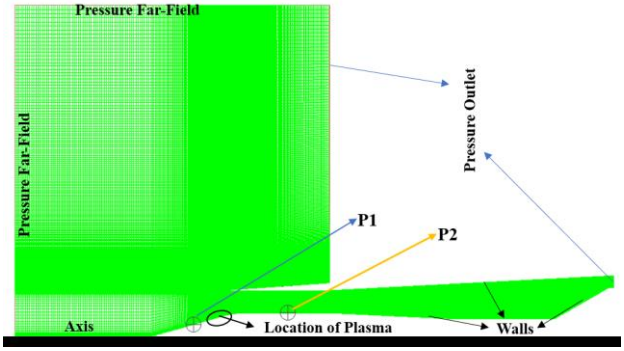

Fig. 2 Grid distribution and the boundary conditions

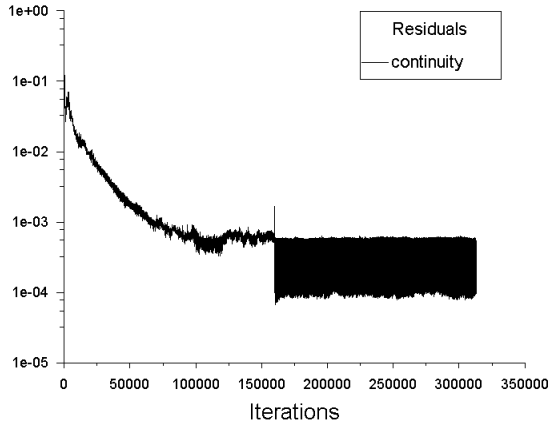

Fig. 3 Residual plot

location where a constant monitoring of pressures were made for the purpose of FFT. The continuity residuals were monitored and is shown in Fig. 3.

Grid independency test has been done for three various grids of coarse (50k cells), medium (100k cells) and fine mesh (200k cells). Simulations with all these grids were made, and a comparison of all these grid cases showing the pressure distribution on the central spike is presented in Fig. 4 with a throttled intake exit (TR=0.48). It is observed that medium mesh (100k cells) is preferred for further axisymmetric simulations, and the similar option was adopted for the further simulations.

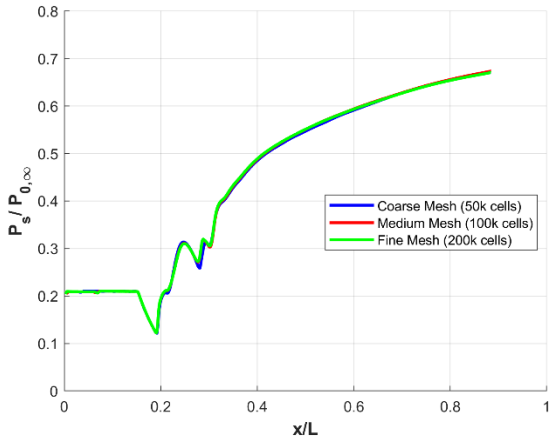

Fig. 4 Grid sensitivity test at a throttled exit of TR = 0.48.

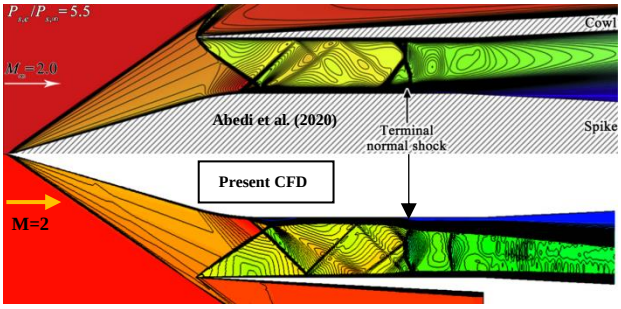

Fig. 5 Comparison for a typical throttled exit of TR 0.48 with the literature (Abedi et al., 2020) having back pressure ratio of 5.5

In this scenario, the flow field computation involves air as an ideal gas, and the fluid's viscosity is determined using Sutherland's three-coefficient method. Initial simulations were made with steady equations and then unsteady simulations were started. The time step size of $1e^{-06}$ was used, considering a reference time of T = 0.1s. Each time step involves 30 iterations to advance the simulation.

A typical test scenario from Abedi et al. (2020) has been used to compare Mach contour and is presented in Figure 5, which offers qualitative findings for validation purposes. The quantitative comparison between the current computation and the reported pressure distribution is given in Figure 6. Comparison is made with a present configuration TR of 0.48 corresponding to a back exit pressure of 5.5 reported in the literature. The present axisymmetric intake has been scaled down to meet the supersonic wind tunnel's current condition requirements.

2.2 Plasma Actuator

For the present tests intake was operated with plasma at the spike side i.e. just upstream of throat of the air intake as shown in Fig. 2.

Dielectric Barrier Discharge (DBD) type of plasma actuation works with the principal of two metal electrodes which are overlapped and spaced apart by a dielectric substance. When the electrodes receive an adequate high supply voltage, the electric field gradient produces ionised air, or plasma, which exerts a body force on the adjacent

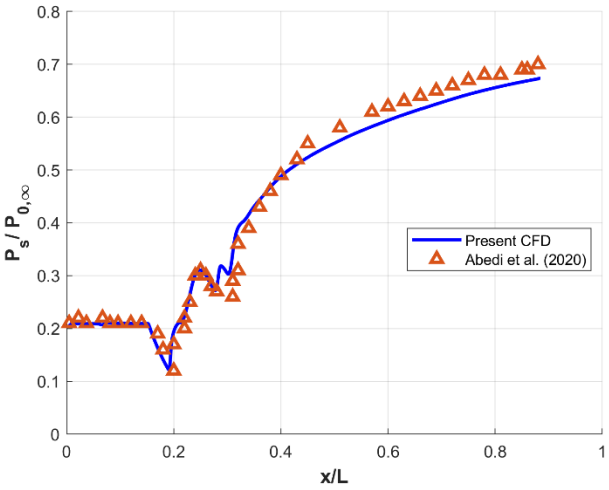

Fig. 6 Comparison of spike pressure distribution at TR=0.48, with the literature having back pressure ratio of 5.5 at exit.

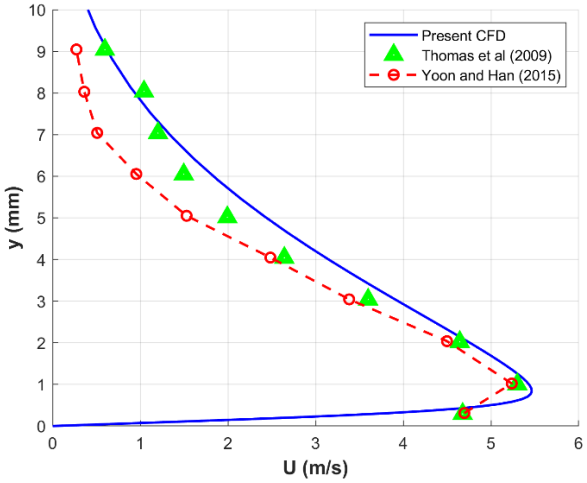

Fig. 7 Comparison of the velocity profiles at x = 38.1 mm downstream of the plasma actuator for a typical case

air. The whole concept has been simulated using a User Defined Function (UDF) integrated with ANSYS Fluent to generate the actuation of plasma by incorporating a body force added as a source term to the momentum equation. The actuator energy is being correlated with this momentum source. This technique of simulating plasma actuation has been adopted from Yoon and Han (2015). To confirm the technique a validation test has also been performed using the test condition from Yoon and Han (2015) before implementing to the present intake model.

Figure 7 shows the comparison of the presently simulated plasma model with the reported computed results of Yoon and Han (2015) and experimental results of Thomas et al. (2009) at a location 38.1 mm downstream distance from the plasma.

After getting a good comparison similar model has been used for the present intake simulation. The protruded portion of the exposed electrode provided an additional

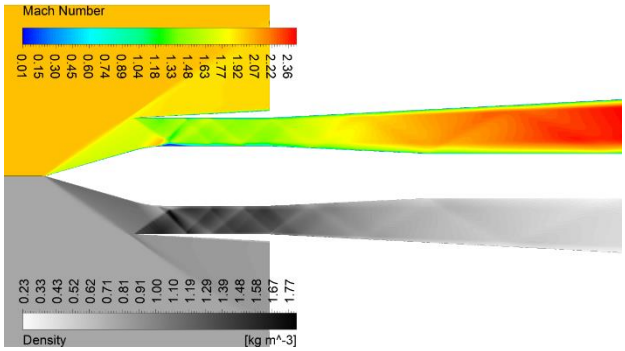

Fig. 8 Mach and density contour at TR 0

shock while implementation, hence it was inscribed within the intake spike body to make the situation flushing with the surface.

Plasma activation can infuse energy into the flow, perhaps reenergizing the boundary layer and improving air mixing within the intake. This could affect shock wave stability and lower the possibility of buzz.

3 RESULTS AND DISCUSSIONS

Initially the results are discussed for the supercritical operation of the intake, which displays the pressure distribution over the spike surface of the axisymmetric air intake at Mach 2. The subcritical operations of the air intake are discussed next which covers the intake buzz condition as well. At the end the impact of plasma actuators at subcritical conditions are discussed.

3.1 Supercritical Operation of Intake:

Free Flow Exit Condition (TR=0):

The operation with TR=0 corresponds to plug, which is so adjusted as to have A_e nearing to A_c. A steady operation is reached after the solution convergence with only oblique shocks external and internal to the intake with a shock on lip condition as per the design consideration. Figure 8 shows the qualitative Mach and density contour showing the entire supersonic flow throughout the internal duct.

Supercritical Condition (TR = 0.48):

The supercritical operation could be simulated by a typical plug arrangement so that the throttle ratio TR becomes 0.48 corresponding to A_e = 52.17 mm^2. it is observed that during supercritical operation, system of shocks are swallowed inside of intake so that there is no spillage of air and still gives a higher mass flow rate similar to the free flow exit condition. For supercritical operation of intake a normal shock stands in the internal duct and finds a suitable position depending on the TR. The flow behaviour in case of such operation is complex because of shock-shock interaction, shock wave boundary layer interaction leading to reduction of pressure recovery of intake.

As we gradually move the conical plug inside the air intake, the static pressure builds up inside the intake,

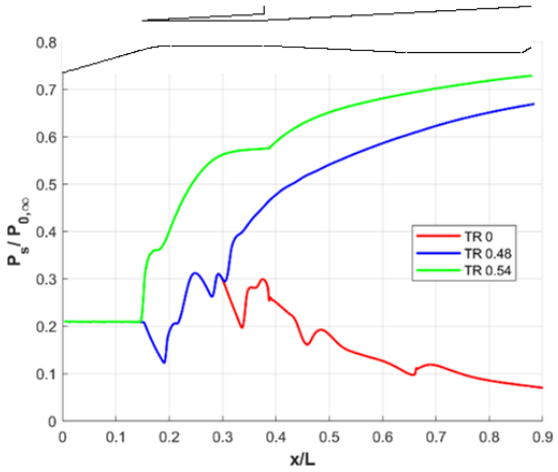

Fig. 9 Spike pressure distributions at various TR

shifting the terminal shock location upstream, similar to the situation presented earlier in Fig. 5.

The critical operating of intake occurs as the most efficient design condition of the intake operation and is achieved by a suitable positioning of the exit plug. The terminal normal shock which existed for supercritical operation at the internal duct of the intake, now ideally should be at a location of the minimum area of the duct which is called as the throat of the intake at a typical TR value. This operating condition should contribute to a stable location of terminal normal shock giving the highest pressure recovery retaining the maximum mass flow rate.

Figure 9 displays the pressure variation on the spike body over an axisymmetric intake for various throttling ratios ranging from supercritical to critical conditions, corresponding to the shock structure depicted in Figs 5, and 8. The static pressure distribution is normalised with respect to the freestream total pressure $P_{0,\infty}$. Fig. 9 depicts the pressure at different throttle ratios for a freestream Mach number of 2. As the throttling ratio increases, the normal shock position moves upstream.

Performance Evaluation of Intake:

Total Pressure Recovery (TPR) is expressed as the ratio of the average exit total pressure $(P_{0e})_{avg}$ to the freestream total pressure ($P_{0\infty}$), as per equation

$$\text{TPR} = \frac{(P_{0e})_{avg}}{P_{0\infty}} \qquad (2)$$

3.2 Subcritical Operation of Intake

In subcritical operation, shock system pops out of intake and normal shock wave is formed outside of cowl lip. The spillage occurs through the cowl lip and reduces the air mass flow rate through the intake duct and hence mass flow rate inside the engine is reduced.

Further movement of the plug inside the intake makes the throttle ratio to increase where the pressure builds up enormously, which in turn expels the normal shock outside the intake. As we further increase the plug inside the intake, a consequent rapid oscillations of the shockwaves occur. This oscillation starts from the terminal shock being just outside the cowl tip to the shock system

inside the internal duct with a to-and-fro motion of terminal shock. This could be attributed to big buzz where the air intake performance is greatly reduced.

Buzz Cycle Description: (TR 0.62)

TR 0.62 describes the buzz cycle of intake operation which is presented by the density contour overlapped with streamline traces the flow features and is presented in Fig. 10. At time t=0.0729 s, the terminal shock is exactly at the cowl lip, which refers to the critical operation of the air intake for a very short period, where it is supposed to have a mass flow rate to be maximum. After some time, this terminal shock moves inside the intake, which refers to the supercritical operation of the intake, where pressure begins to fall. As soon as the normal shock moves downstream, high pressure builds up due to higher throttling, reflects back the system of shock upstream at t=0.0732 s, which deflects the oncoming normal shock wave to move upstream at t=0.0735 s. Based on Dailey's criterion, a boundary layer creates at the spike side of the air intake, which moves more upstream at t=0.0738 s, affecting the mass flow rate of the intake. As the flow separation grows and moves upstream, the terminal normal shock is expelled out of the intake. Strong bow shockwave forms ahead of the cowl lip of the air intake, referring to a subcritical operation. This expelled normal shockwave later forms a strong conical shockwave at t=0.0741 s as it progresses towards the spike part of the air intake. As the conical shockwave reaches most upstream part of the spike there is a discontinuity of pressure at t=0.0744 s due to large flow separation. When the separation region collapses, at t=0.0747 s the conical shockwave retreats back downstream of the intake, thus forming a lambda shockwave. This lambda shockwave becomes almost terminal shock when the incoming shock approaches the intake throat at t=0.075 s; hence the separation zone decreases, and the cycle repeats.

To quantify the shock-related unsteadiness generated by plug insertion for different throttling ratios in the subcritical condition, unsteady pressure fluctuations have been monitored near the spike (x/L = 0.12) and throat (x/L = 0.29) of the axisymmetric air intake as shown in Fig. 11. Fast Fourier Transform (FFT) of Amplitude from the pressure signal has been obtained for the two points P1 and P2, and are compared presented in Fig. 11. For the subcritical conditions: TR 0.58, TR 0.62, and TR 0.68, Fig. 11(a, c, and e) represents the pressure fluctuations of the two points at the spike body of the air intake. This figure clearly shows the harmonic and high amplitude variations of the pressure signals. The amplitude of the pressure oscillations at P1 is greater than that of P2. FFT analysis at the three TR has been presented in Fig. 11 (b, d, and f). The broadband spectra for all the throttling cases are exhibited with higher amplitudes. The fundamental frequency for the three throttling ratios has been represented in Fig. 11 (b, d, and f). Hence Fig. 11 clearly shows the initiation of the buzz, which is due to Dailey phenomena.

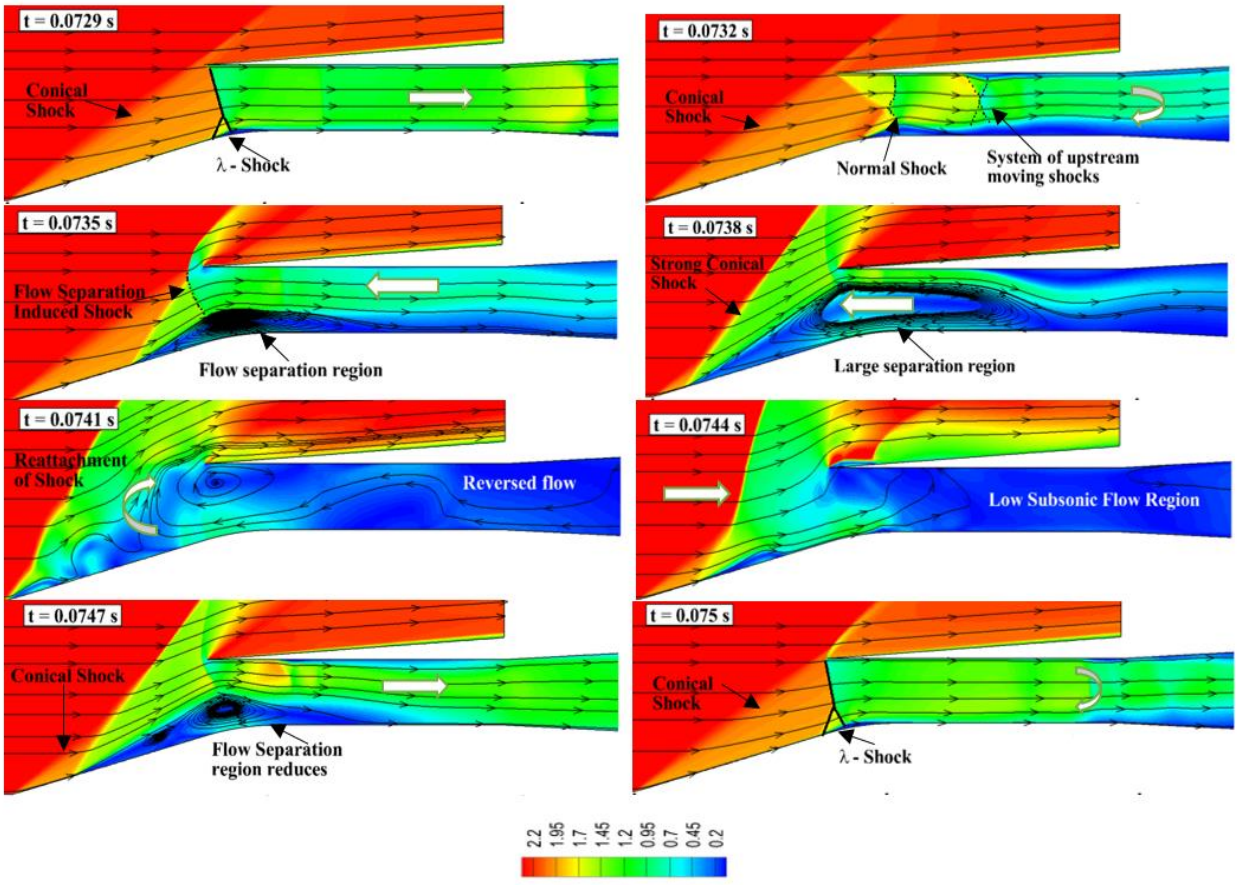

Fig. 10 Streamline traces on Mach contour for TR=0.62, showing one cycle of buzz with Δt in between frames as 0.0003

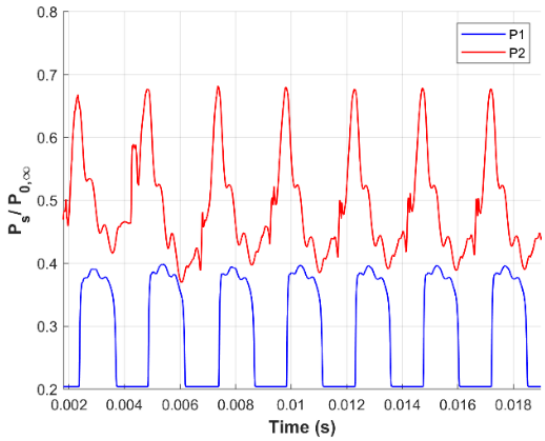

(a) Pressure time history with TR=0.58

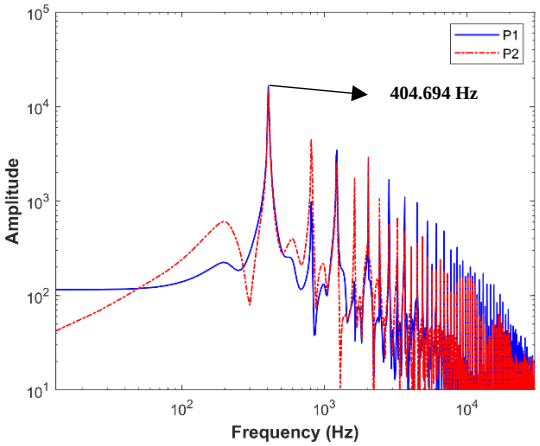

(b) Pressure spectrum with TR=0.58

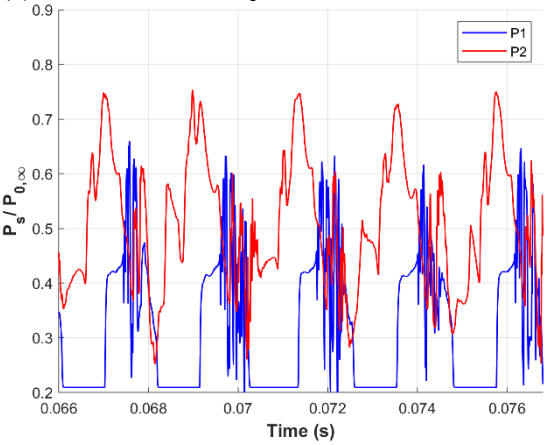

(c) Pressure time history with TR=0.62

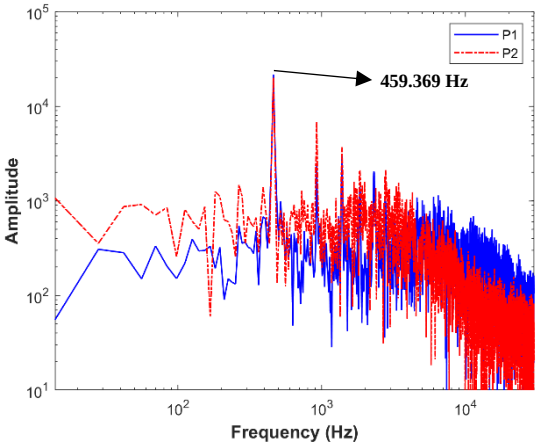

(d) Pressure spectrum with TR=0.62

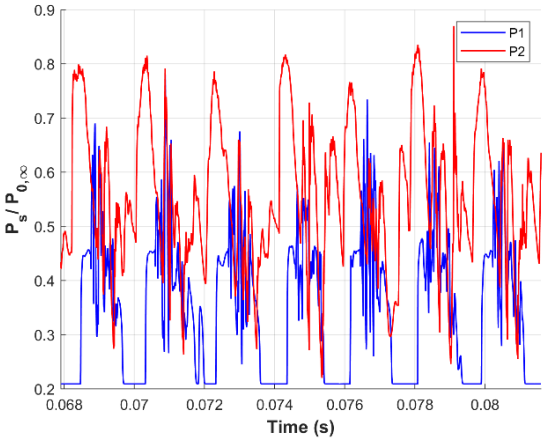

(e) Pressure time history with TR=0.68

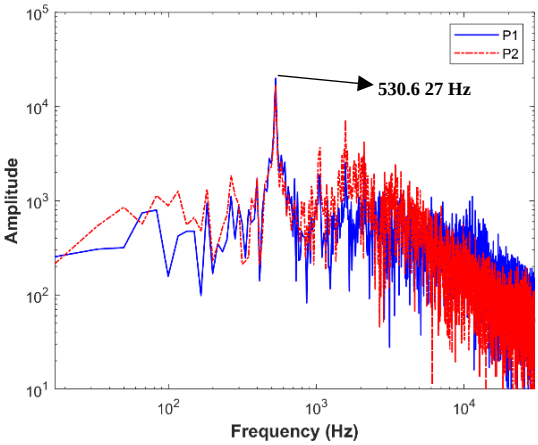

(f) Pressure spectrum with TR=0.68

Fig. 11 Pressure time history and FFT at P1&P2 on spike at various throttling ratio

3.3 Plasma on Analysis at Subcritical Conditions

In the course of flight, individual air vehicles manifest distinct Mach numbers. Consequently, integrating a plasma source into the flow field of high-speed intakes during off-design conditions holds the potential for beneficial effects. This section provides a numerical study conducted under three distinct Plasma Power Density (PPD) scenarios, each corresponding to a different throttle ratio.

Illustrated in Fig. 2 is the spatial location of plasma at x/L = 0.12, featuring a horizontal span of 5 mm. Notably, this spatial location remains consistent across all investigated scenarios, upon the applied Plasma Power Density.

The influence of applying a plasma actuator on the intake flow field:

A typical throttling ratio of TR = 0.58 is selected to explain the influence of plasma (with a typical Plasma Power Density [PPD] of 14 MW/m^2) with the help of instantaneous pictures obtained from the numerical simulation. Figure 12(a-i) shows the instantaneous images which are the superposition of streamlines over its Mach contour to signify the flow characteristics immediately after the plasma is activated. Figure 12(a) signifies intake

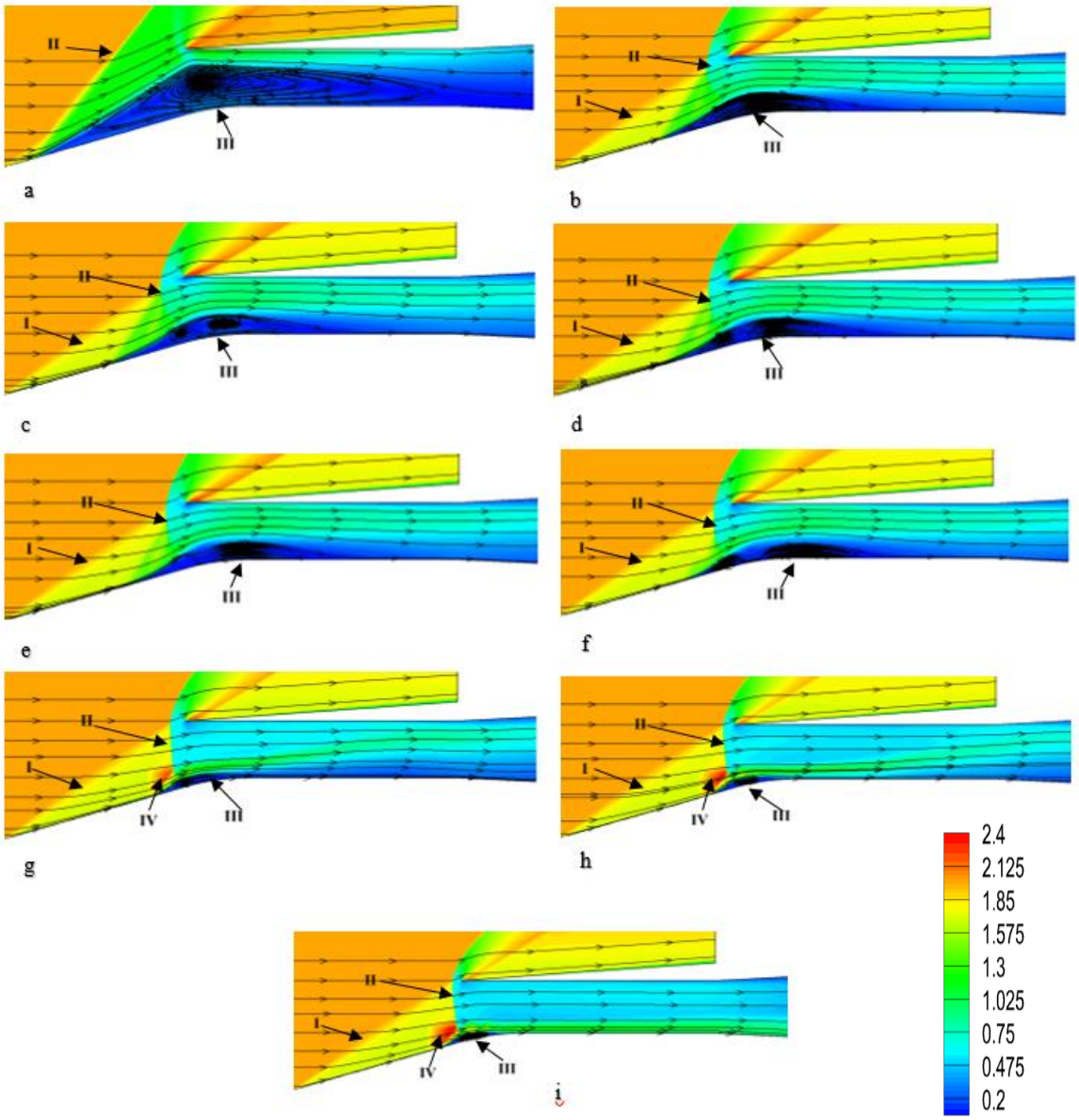

Fig. 12 Mach contours with influence of plasma at PPD 14 MW/m^2 at TR 0.58

(I-Conical Shock, II-Flow Separation Induced Shock, III- Flow Separation Region, IV-Plasma Region)

operation at a time t = 0.062 s with a huge flow separation at the entry of internal duct of intake which is one of the instantaneous moments of intake buzz. Figure 12 (b) shows the contours at time t = 0.069 s, when the plasma is just activated. With the subsequent time progress as seen from Fig. 12(c)–(i), it is observed that the separation and the distorted flow inside the duct subsides and slowly becomes steady at the end of its cycle. The plasma actuator plays a role of boundary layer energizer and modifies the flow structure inside the intake duct. After the plasma impact it is seen that the terminal normal shock in the form of a bow shock just at the entry of intake duct ceases to oscillate on the spike and it becomes steady and stable.

3.3.1 PPD at 7 MW/m^2

Simulations of plasma with a power of 7 MW/m^2 was executed, and the monitoring points describe the advantages gained due to the operation presented in Fig. 13. Pressure time history at P1 location indicates reduced amplitude of pressures as observed through Fig. 13 (a) for operation with plasma. The data's corresponding FFT also suggests a decrease in amplitude but retains the frequency of occurrence nearing the base value obtained for no plasma. Table 1 presents the results obtained for all the throttle ratios tested and plasma power operated with. It can be observed clearly from the table that the plasma power of 7 MW/m^2 may have been instrumental in decreasing the pressure amplitude, but the frequency of oscillation does not change or alter its characteristics.

3.3.2 PPD at 14 MW/m^2

The simulation was carried out with a plasma power of 14 MW/m^2; the benefits obtained are depicted in Fig. 14. The pressure time history at point P1 exhibits a linear trend during the plasma process, as seen in the accompanying image. However, when looking at TR 0.68 in Fig. 15(a), it is clear that the pressure time history has no substantial amplitude reduction at point P1. Instead, as

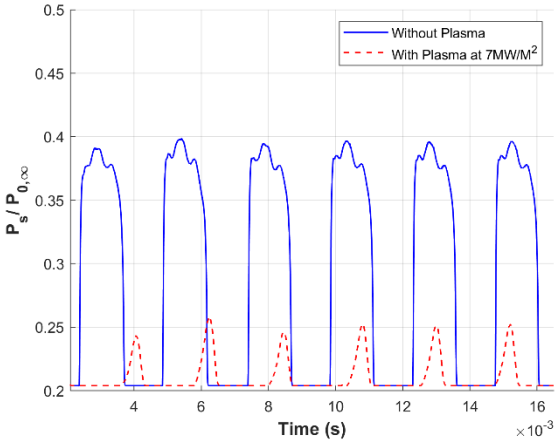

(a) Pressure time history at P1

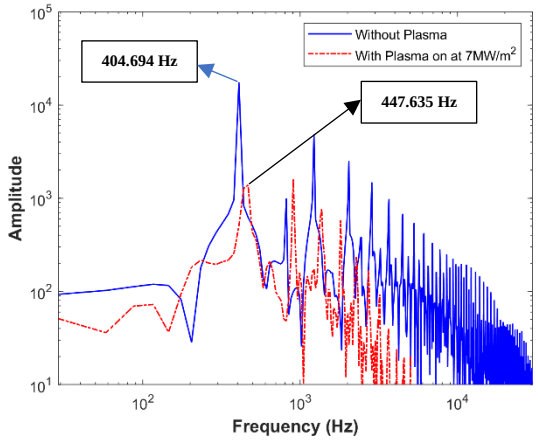

(b) Pressure spectra at P1

Fig. 13 Comparison of operation with plasma (7 MW/m^2) and without plasma at point P1 with a throttling ratio of TR 0.58

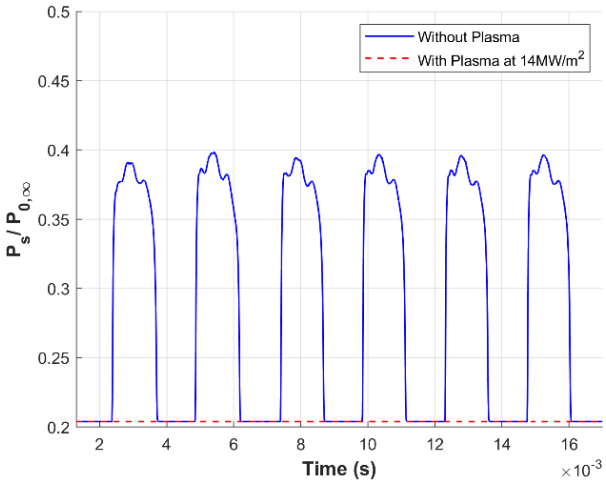

Fig. 14 Comparison of operation with plasma (14MW/m^2) and without plasma at point P1 with a throttling ratio of TR 0.58

seen in Fig. 15(b), a slight shift in frequency reduction is observed. Table 1 summarizes the observations, revealing that the intake achieves stabilization with a plasma power

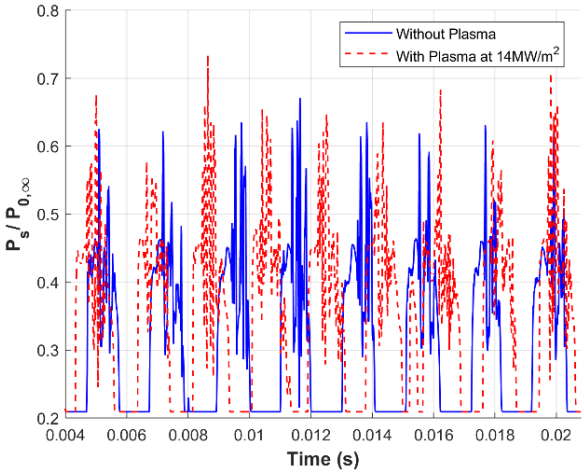

(a) Pressure time history at P1

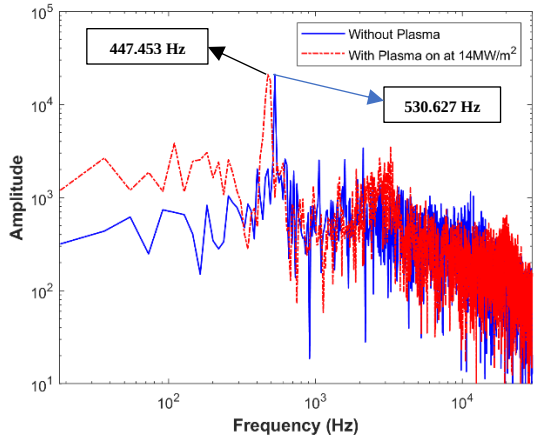

(b) Pressure spectra at P1 Figure

Fig. 15 Comparison of operation with plasma (14 MW/m^2) and without plasma at point P1 with a throttling ratio of TR 0.68

of 14 MW/m^2 at TR=0.58 and 0.62. This suggests that pressure oscillations did not occur during the first two throttling ratios, indicating a favorable and controlled operational state. The oscillation frequency is lowered by roughly 83 Hz at increased throttling, i.e. at TR of 0.68.

3.3.3 PPD at 21 MW/m^2

Similarly, simulations were done with a plasma power of 21 MW/m^2; the results are shown in Fig. 16 as a monitoring point. Notably, there are no pressure oscillations during plasma operation in the pressure time

history at location P1. Table 1 shows that the intake remains consistently stable over all three throttle ratios, indicating no pressure changes. This shows a positive outcome, implying a consistent and controlled performance under the influence of plasma power.

The Plasma Power's Overall Effectiveness

This study revealed that employing plasma with specific power can alter supersonic intake buzz characteristics in two key ways. First, it postpones buzz initiation, enhancing engine reliability. Second, it reduces the range of oscillations, a significant advantage.

Table 1 Typical buzz oscillation frequency (Hz) for different Plasma Powers

Mach	TR	No Plasma Condition	Plasma on condition		
			7MW/m^2	14MW/m^2	21MW/m^2
2	0.58	404.694 Hz	447.635 Hz	Stable	Stable
	0.62	459.369 Hz	441.696 Hz	Stable	Stable
	0.68	530.627 Hz	530.623 Hz	447.453 Hz	Stable

Table 2 Performance parameters for the various throttling ratios (Stable condition) at Mach 2

TR	Condition	Plasma condition	Plasma Power	TPR
0.48	Super critical	Off	-	0.75
0.54	Near-critical	Off	-	0.79
0.58	Buzz	Off	-	0.65
		On	14MW/m^2	0.85
		On	21MW/m^2	0.86
0.62	Buzz	Off	-	0.58
		On	14MW/m^2	0.87
		On	21MW/m^2	0.89
0.68	Buzz	Off	-	0.62
		On	21MW/m^2	0.88

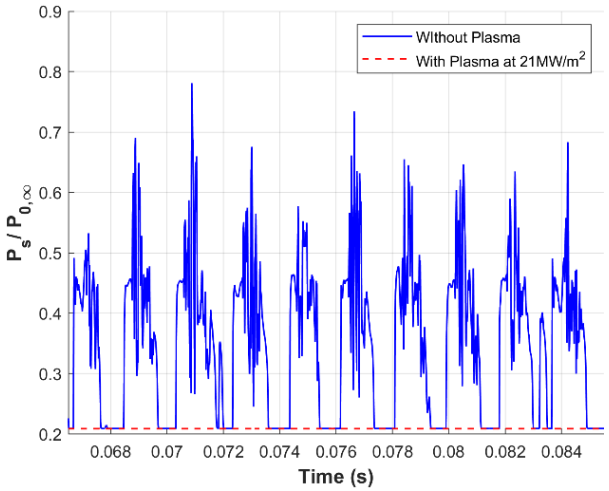

Fig. 16 Comparison of operation with plasma (21 MW/m^2) and without plasma at point P1 with a throttling ratio of TR 0.68

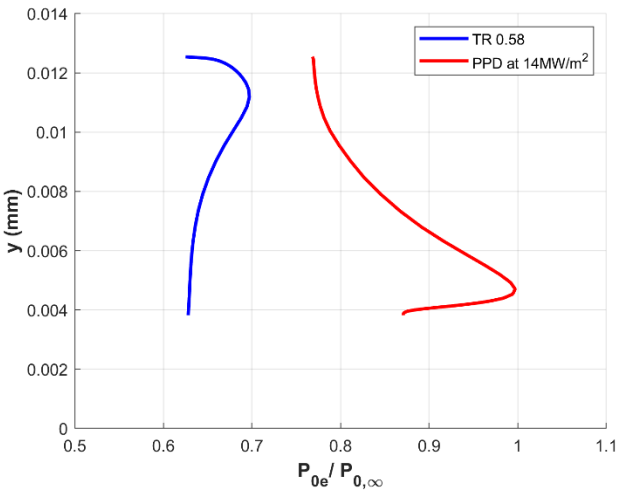

Fig. 17 Plot of average TPR of several samples of one complete oscillation.

Table 2 displays the performance parameters for the range of operating conditions encompassing supercritical to subcritical buzz conditions. The total pressure recovery increased considerably with the inclusion of plasma conditions.

With plasma off condition the instantaneous results show (Fig. 17) distorted behavior and hence as per suggestion the table includes the average Total Pressure Recovery (TPR) of several samples from one complete cycle of oscillation.

4. CONCLUSION

Numerical simulations were made to axisymmetric air-intake designed for Mach 2.0 with an objective to adequately subside the buzz phenomena occurring at subcritical operation of the intake. A mass flow plug at the intake exit was throttled to obtain the different operations of the intake (subcritical, critical and supercritical), and its subsequent threshold values for such operations. The buzz phenomena prevalent at subcritical operation of the intake is demonstrated to obtain the frequency of buzz based on Dailey criterion. Simulation of plasma on the surface of intake could be demonstrated here with 3 PPD of 7, 14, and 21 MW/m^2. Results indicate that plasma has the potential to decrease the buzz intensity and its frequency when applied locally at suitable position on the intake. The intensity of plasma also do play a vital role in the complete alleviation of buzz.

CONFLICT OF INTEREST

The authors declare no conflict of interest to disclose.

AUTHORS CONTRIBUTION

Praveen Kumar obtained his MTech (Aerospace Engineering) from Jawaharlal Nehru Technological University (JNTU), Hyderabad, in 2020. He works at BIT

Mesra as a Research Scholar in the Department of Space Engineering and Rocketry. Shock waves and boundary control are among the topics of his research. His dissertation includes the current investigation. **Sudip Das** obtained his PhD in engineering from BIT Mesra and Post-Doc from Technion, Israel Institute of Technology. He is employed by BIT Mesra as a professor. To his credit, he has over 130 publications in conference proceedings and journals. Among many other topics, his research focuses on unsteady aerodynamics, shock boundary layer interaction, and high speed flows. The Indian Society for Technical Education, the Institution of Engineers (I), the Aeronautical Society of India, and the Society of Fluid Mechanics and Fluid Power are among the organizations he adheres to.

REFERENCES

Abedi, M., Askari, R., Sepahi Younsi, J., & Soltani, M. R. (2020). Axisymmetric and three-dimensional flow simulation of a mixed compression supersonic air inlet. *Propulsion and Power Research*, 9(1), 51-61. https://doi.org/10.1016/j.jppr.2020.01.002

Chen, H., & Tan, H. J. (2019). Buzz flow diversity in a supersonic inlet ingesting strong shear layers. *Aerospace Science and Technology*, 95, https://doi.org/10.1016/j.ast.2019.105471.

Chen, H., Tan, H. J., Zhang, Q. F., & Zhang, Y. (2017). Buzz flows in an external-compression inlet with partially isentropic compression. *AIAA Journal*, 55, (12), 4286–4295. https://doi.org/10.2514/1.J056066.

Chen, H., Tan, H. J., Zhang, Q. F., & Zhang, Y. (2018). Throttling process and buzz mechanism of a supersonic inlet at overspeed mode. *AIAA Journal*, 56(5), 1953–1964. https://doi.org/10.2514/1.J056674.

Dailey, C. L. (1954). *Supersonic Diffuser Instability* [PhD. dissertation, California Inst. of Technology], Pasadena, CA. https://doi.org/10.2514/8.3452

Falempin, F., Firsov, A. A., Yarantsev, D. A., Goldfeld, M. A., Timofeev, K., & Leonov, S. B. (2015). plasma control of shock wave configuration in Off-Design mode of M = 2 inlet. *Experiments in Fluids*, 56(3), 2–11. https://doi.org/10.1007/s00348-015-1928-4

Ferrero, A. (2020). Control of a supersonic inlet in off-design conditions with plasma actuators and bleed. *Aerospace*, *7*(3), 32. https://doi.org/10.3390/aerospace7030032

Ferri, A., & Nucci, L. M. (1951). *The origin of aerodynamic instability of supersonic inlet at subcritical condition.* NACA RM-L50K30. https://ntrs.nasa.gov/citations/19930086483

Ganiev, Y. C., Gordeev, V. P., Krasilnikov, A. V., V. I. Lagutin, V. I., Otmennikov, V. N., & Panasenko, A. V. (2000). Aerodynamic drag reduction by plasma and hot-gas injection. *Journal of Thermophysics and Heat Transfer* *14*(1), 10–17. https://doi.org/10.2514/2.6504.

Kandala, R., & Candler, G. V. (2004). Numerical studies of laser-induced energy deposition for supersonic flow control. *AIAA Journal*, *42*(11), 2266–2275. https://doi.org/10.2514/1.6817.

Kumar, P., & Das, S. (2023, September 1-2). Influence of plasma during supersonic intake buzz. *36th National Convention of Aerospace Engineers (NCAE-2023)*, Karnataka State Centre, Bengaluru. https://www.researchgate.net/publication/373717996_Influence_of_Plasma_during_Supersonic_Intake_Buzz

Kwak, E., & Lee, S. (2013). *Numerical study of the effect of exit configurations on supersonic inlet buzz*. 31st AIAA Applied Aerodynamics Conference, San Diego, California. https://doi.org/10.2514/6.2013-3025.

Lee, H. J., Lee, B. J., Kim, S. D., & Jeung, I. (2011). Flow characteristics of small sized supersonic inlets. *Journal of Propulsion and Power, 27*(2), 306e318. https://doi.org/10.2514/1.46101.

Maadi, S. R., & Sepahi-Younsi, J. (2021). Effects of bleed type on the performance of a supersonic intake. *Experimental Thermal and Fluid Science*, *132*, 110568. https://doi.org/10.1016/j.expthermflusci.2021.110568

Macheret, S. O., Shneider, M. N., & Miles, R. B. (2004). Scramjet inlet control by off-body energy addition: A virtual cowl. *AIAA Journal*, *42*(11), 2294–2302. https://doi.org/10.2514/1.3997.

Mattingly, J. D., & Von Ohain, H. (2006). *Elements of propulsion: gas turbines and rockets.* AIAA Reston, AIAA Education Series, USA. https://doi.org/10.2514/4.103711

Nagashima, T., Obokata, T., & Asanuma, T. (1972). *Experiment of supersonic air intake buzz.* Institute of Space and Aeronautical Science of Tokyo, Japan, Rept. No. 481, 37-7, 165-209. https://jaxa.repo.nii.ac.jp/record/34639/files/SA2406802.pdf

Patel, M. P., Cain, A. B., Nelson, C. C., Corke, T. C., & Matlis, E. H. (2012). *Shock generation and control using DBD plasma actuators*. SBIR Phase I Final Report. NASA/CR—2012-217448. https://ntrs.nasa.gov/api/citations/20120011134/downloads/20120011134.pdf

Seddon, J., & Goldsmith, E. L. (1985). *Intake Aerodynamics*. Collins Publications. https://doi.org/10.1017/S0001924000015359

Sepahi-Younsi, J., & Esmaeili, S. (2020). Performance enhancement of a supersonic air intake by applying a heat source. *Journal of Aerospace Engineering. 33*(5), 04020048, https://doi.org/10.1061/(ASCE)AS.1943-5525.0001170

Shyy, W., Jayaraman, B., & Andersson, A. (2002). Modeling of glow discharge-induced fluid dynamics.

Journal of Applied Physics, *92*(11), 6434-6443. https://doi.org/10.1063/1.1515103

Soltani, M. R., & Sepahi-Younsi, J. (2015). Buzz cycle description in an axisymmetric mixed-compression air intake. *AIAA Journal*, *54*(3), 1040-1053. https://doi.org/10.2514/1.J054215

Soltani, M. R., Daliri, A., Younsi, J. S., & Farahani, M. (2016). Effects of bleed position on the stability of a supersonic inlet. *Journal of Propulsion and Power*, *32*(5), 1153-1166. https://doi.org/10.2514/1.B36162

Thomas, F. O., Corke, T. C., Iqbal, M., Kozlov, A., & Schatzman, D. (2009). Optimization of dielectric barrier discharge plasma actuators for active aerodynamic flow control. *AIAA journal*, *47*(9), 2169-2178. https://doi.org/10.2514/1.41588.

Trapier, S., Duveau, P., & Deck, S. (2006). Experimental study of supersonic inlet buzz. *AIAA Journal*, *44* (10). https://doi.org/10.2514/1.20451.

Trapier, S., Duveau, P., & Deck, S. (2008). Delayed detached-eddy simulation and analysis of supersonic inlet buzz. *AIAA Journal*. https://doi.org/10.2514/1.32187.

Vivek, P., & Mittal, S. (2009). Buzz instability in a mixed-compression air intake. *Journal of Propulsion and Power,* *25*(3), 819–822. https://doi.org/10.2514/1.39751.

Yoon, J. S., & Han, J. H. (2015). Semiempirical thrust model of dielectric barrier plasma actuator for flow control. *Journal of Aerospace Engineering*, *28*(1), 04014041. https://doi.org/10.1061/(ASCE)AS.1943-5525.000035.